Aggregation state of melittin in lipid vesicle membranes

Edgar John and Fritz Jähnig
Max-Planck-Institut für Biologie, Abteilung Membranbiochemie, Corrensstrasse 38, D 7400 Tübingen, Germany

ABSTRACT We have performed time-resolved fluorescence energy transfer measurements using melittin as donor and a modified melittin as acceptor. The melittin molecules were bound to fluid vesicle membranes of dimyristoylphosphatidylcholine. Analysis of the temporal decay of the energy transfer and of its variation with the donor and acceptor concentrations led to the conclusion that melittin in fluid membranes is usually monomeric. Only at the high melittin/lipid molar ratio of 1/200 and high ionic strength evidence for aggregation was obtained, the percentage of aggregated melittin molecules being of the order of 10%. The shortcomings of previous steady-state measurements of fluorescence energy transfer between melittin molecules are discussed.

INTRODUCTION

Melittin has been studied extensively as a model for membrane proteins, especially for voltage-gated pores (Dempsey, 1990). Still, however, the structure of melittin in membranes has not been fully characterized. Agreement has been reached about the α-helix conformation of the 26-residue polypeptide chain (Vogel and Jähnig, 1986; Brauner et al., 1987; Bazzo et al., 1988; Inagaki et al., 1989). But on the orientation of the α-helix relative to the membrane plane conflicting results have been reported (Vogel, 1987; Brauner et al., 1987; Stanislawski and Rüterjans, 1987; Altenbach and Hubbell, 1988), and the same is true for the state of aggregation of the helices (Vogel and Jähnig, 1986; Hermetter and Lakowicz, 1986; Talbot et al., 1987; Schwarz and Beschiaschvili, 1989).

The studies on the orientation of the melittin helices fall into two classes. Those which used stacks of oriented membranes and detected the orientation of the helices via circular dichroism or infrared spectroscopy found a predominant orientation parallel to the membrane normal (Vogel, 1987; Brauner et al., 1987) while those which used vesicle membranes and detected the accessibility of certain amino acid residues by electron spin resonance (ESR) or nuclear magnetic resonance (NMR) spectroscopy obtained evidence for the helices lying flat on the membrane surface (Stanislawski and Rüterjans, 1987; Altenbach and Hubbell, 1988). The latter orientation would be more compatible with the amphiphilic character of the helices as long as they exist as monomers. The membrane-spanning orientation, on the other hand, would probably require an aggregation of the helices with their hydrophilic sides facing each other and thus shielding them from the lipids. The simplest way out of the dilemma with the orientation of the melittin helices would be to postulate a different orientation in stacked membranes and in vesicle membranes. It might be that packing of the stacked bilayers with low amounts of water between the bilayers forces the helices to enter the membrane and become membrane spanning, accompanied by an aggregation.

The situation with the aggregation studies is even more complicated because contradictory results have been obtained using the same systems and the same technique for detection of aggregation. All studies used vesicle membranes and observed fluorescence energy transfer (FET) between melittin as donor and an appropriately modified melittin as acceptor. FET was always detected in steady-state measurements. Vogel and Jähnig (1986) came to the conclusion that melittin in membranes forms tetramers in a concentration-dependent manner, while Talbot et al. (1987) reported that aggregation occurs only at high salt concentration, and Hermetter and Lakowicz (1986) as well as Schwarz and Beschiaschvili (1989) found no evidence for aggregation. The studies differ in the analysis of the data. In some cases, the direct absorption by acceptor molecules has been taken into account but not in others. Similarly, in some cases the contribution to FET due to the random distribution of donors and acceptors has been considered but not in others. The latter effect may be of special importance in membranes, since the effective concentration of donors and acceptors in a two-dimensional membrane may be much higher than in a three-dimensional solution.

In this situation, we decided to perform FET measurements in a time-resolved manner on melittin in vesicle membranes. Time-resolved measurements have the advantage that any influence of direct absorption due to

0006-3495/91/08/319/10 $2.00

acceptor molecules is excluded and, furthermore, the distinction between FET due to a random distribution or aggregation can be made on the basis of their different time behavior. Our conclusion is that, in vesicle membranes, melittin is usually monomeric, only at high salt concentration and at melittin/lipid molar ratios above 1/200, it aggregates to some extent. This is in contrast to previous FET studies indicating aggregation of melittin in vesicle membranes (Vogel and Jähnig, 1986; Talbot et al., 1987). The shortcomings of these studies will be discussed.

MATERIALS AND METHODS

Chemicals

Dimyristoylphosphatidylcholine (DMPC) was purchased from Fluka (Neu Ulm, Germany). P-terphenyl (PTP) was obtained from Sigma (Munich, Germany), 1,6-diphenyl-1,3,5-hexatriene (DPH) from Aldrich (Steinheim, Germany) and 2-hydroxy-5-nitrobenzylbromide (HNB) from Serva (Heidelberg, Germany).

All solvents were of spectroscopic grade or classified "for preparative HPLC" and were purchased from Merck (Darmstadt, Germany).

Purification and chemical modification of melittin

Melittin was purchased from Serva and purified according to the procedure of Wille (1989). After purification no phospholipase activity could be detected. It was stored as a 1-mM stock solution in Milli-Q water at −20°C. The amount of melittin was determined by weight or by extinction using $\epsilon_{280} = 5{,}570\ M^{-1}\ cm^{-1}$ (Quay and Condie, 1983).

Chemically modified melittin, henceforth called A-melittin, was prepared by means of the Koshland reaction using HNB, as described by Habermann and Kowallek (1979). This yields a nonfluorescent derivative of the single tryptophan residue of melittin. At pH 4.5, the absorption spectrum of the modified tryptophan shows a peak at 310 nm, which is shifted to 410 nm by increasing the pH value to pH ≥ 10. A-melittin was purified by fast protein liquid chromatography (FPLC) on a reversed phase column (Pro-RPC 5/10; Pharmacia Fine Chemicals, Uppsala, Sweden). 0.3 mg A-melittin per run were eluted with a linear gradient from 0 to 100% acetonitrile in 0.1% trifluoroacetic acid over 20 min at 1 ml/min. After lyophilisation A-melittin was stored as a 1-mM stock solution in Milli-Q water at −20°C. The amount of A-melittin was determined by weight and by extinction at pH > 10.0 using $\epsilon_{410} = 18{,}000\ M^{-1}\ cm^{-1}$ (Horton and Koshland, 1967). Purified A-melittin contained less than 5% unmodified melittin, shows the same electrophoretic behavior (Vogel and Jähnig, 1986) and a similar lytic activity (Habermann and Kowallek, 1970) as native melittin.

Sample preparation

To prepare lipid vesicles, an appropriate amount of DMPC was dissolved in buffer (10-mM potassium hydrogen phosphate (KPP), pH 7.4, with or without 1 M sodium chloride) and tip sonicated for about 10 min, followed by centrifugation at 10,000 *g* for 10 min to remove metal debris from the tip sonication. Before use, the vesicles were stored for about 1 h, below and above the phase transition temperature.

To prepare vesicles with melittin, melittin was added from the stock solution to the preformed vesicles at 36°C and incubated for at least 30 min. The final melittin concentration in all experiments was 5 μM. A-melittin was titrated to the vesicles from the stock solution and incubated for at least 10 min. After this time no variation in the fluorescence signal could be detected.

To measure FET with DPH as acceptor, DPH was added to the vesicles from a 1-mM stock solution in dimethylsulfoxide. The volume of the added stock solution at the highest DPH concentration was 0.5% of the sample volume.

To each sample, a control sample was prepared without melittin and titrated with A-melittin or DPH in the same way as the samples.

Investigations of the samples by electron microscopy showed that almost all vesicles were unilamellar with diameters between 50 and 200 nm.

The sample used as fluorescence standard was a 5-μM solution of PTP in cyclohexane. The control sample here was cyclohexane.

Fluorescence measurements

Steady-state fluorescence measurements were performed on a Perkin-Elmer (Norwalk, CT) MPF-3 spectrometer. Trp fluorescence was excited at $\lambda_{ex} = 290$ nm. The slit width was set to 4 nm. The steady-state intensities I^{ss} and I_0^{ss} obtained in the presence and absence of acceptor molecules, respectively, provide the relative quantum yield as $\phi_r = I^{ss}/I_0^{ss}$.

The apparatus for time-resolved fluorescence measurements has been described previously (Best et al., 1987). A mode-locked argon-ion laser synchronously pumps a cavity-dumped dye laser to generate light pulses at a repetition rate of 4 MHz. To excite Trp fluorescence, rhodamine 6G was used as laser dye and the wavelength was set, after frequency doubling, to $\lambda_{ex} = 290$ nm. The emission wavelength was selected by a monochromator, $\lambda_{em} = 340$ nm, slit width 9 nm, in combination with a cutoff filter (WG 320/4; Schott Corp., Yonkers, NY). The sample holder could be rotated to bring four different 1 × 1-cm quartz cuvettes into the exciting beam. They contained the sample, the control sample, the fluorescence standard sample, and the control sample for the fluorescence standard.

To measure the total fluorescence intensity, the polarizer in the emission light path was set at the magic angle of 54.7°.

Data analysis of the time-resolved fluorescence measurements

The data were analyzed according to the procedure described by Best et al. (1987). The measured intensities of the samples were corrected for background by subtracting the intensities of the control samples, and the intensities thus obtained were deconvoluted using the fluorescence standard PTP with a lifetime of 0.97 ± 0.01 ns (John and Jähnig, 1988). The intensities were fitted by a sum of exponentials,

$$I(t) = \sum_{i=1}^{N} a_i \exp(-t/\tau_i). \quad (1)$$

The partial amplitudes α_i, the average lifetime $\bar{\tau}$, and the relative quantum yield ϕ_r were obtained as

$$\alpha_i = a_i / \sum_{j=1}^{N} a_j,$$

$$\bar{\tau} = \sum_{i=1}^{N} \alpha_i \tau_i,$$

$$\phi_r = \bar{\tau}/\bar{\tau}_0, \quad (2)$$

with $\bar{\tau}$ and $\bar{\tau}_0$ denoting the average lifetime in the presence and absence of acceptor molecules.

General theory of FET

The fluorescence lifetime τ in the presence of energy transfer due to the Förster mechanism from a donor D to acceptors A_i at distances R_i is given by the expression (Förster, 1949),

$$\tau = \tau_0 \left[1 + \sum_{i=1}^{N} (R_0/R_i)^6\right]^{-1}, \quad (3)$$

yielding for the fluorescence intensity,

$$I(t) = \exp\left\{-t/\tau_0 \left[1 + \sum_{i=1}^{N} (R_0/R_i)^6\right]\right\}, \quad (4)$$

with $R_0 = (8.79 \times 10^{-5})\ \chi^2\ n^4\ \phi_0\ J_{DA}$ (Fairclough and Cantor, 1978). Here, χ is the orientation factor for dipole–dipole interaction, n the index of refraction, ϕ_0 the quantum yield of the donor in the absence of acceptors, and J_{DA} the overlap integral between the normalized emission spectrum of the donor and the absorption spectrum of the acceptor (Fig. 1). As shown by Dale and Eisinger (1974), the value of χ can be estimated if the orientational order parameters of donors and acceptors and their mean orientations are known. The order parameter of the Trp side chain of melittin in vesicle membranes was determined previously as $S = 0.55$ (John and Jähnig, 1988). Using this value for the order parameter of both donors and acceptors and, in addition, assuming that the mean orientations of donors and acceptors are parallel, one obtains $\chi^2 = 0.65$. This is close to the value $\chi^2 = 2/3$ expected for a random orientation of donors and acceptors. If, on the other hand, one assumes a perpendicular mean orientation of donors and acceptors keeping $S = 0.55$, one obtains $\chi^2 = 0.25$. In the case of melittin in water, either monomeric or tetrameric, one may assume in lowest approximation that the Trp residues are oriented randomly, hence $\chi^2 = 0.66$. The same assumption may hold for monomeric melittin in membranes. The case of aggregated melittin in membranes may be described better by a parallel mean orientation of the Trp residues with $S = 0.55$, hence $\chi^2 = 0.65$, which closely agrees with the estimated value for monomeric melittin in membranes. The refractive index of lipids is given by $n = 1.4$. The quantum yield ϕ_0 for melittin was determined by comparison with L-tryptophan in water, whose quantum yield is $\phi_0 = 0.14$ (Eisinger, 1969). The overlap integral J_{AD} was derived from the spectra given in Fig. 1 as $J_{AD} = 0.9 \times 10^{-14}\ M^{-1}$ cm^3. Using these numbers one obtains $R_0 = 26 \pm 2$ Å for the pair melittin/A-melittin in water or in membranes at 36°C, pH 7.4. This value is slightly lower than the value $R_0 = 29$ Å of Vogel and Jähnig (1986) which, however, was determined at pH 4.5 where the overlap integral is larger.

Under the same conditions, for the pair, melittin/DPH, one obtains the value $R_0 = 37 \pm 2$ Å.

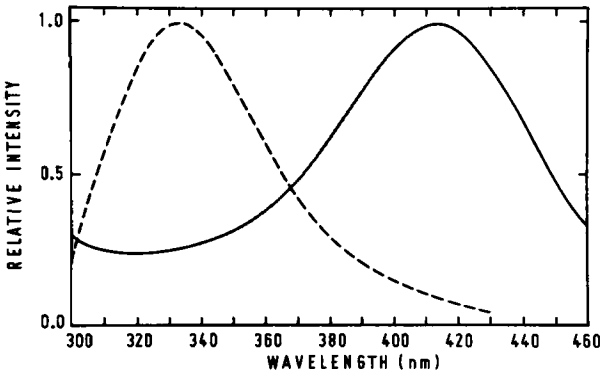

FIGURE 1 Emission spectrum of melittin (---) in vesicle membranes of DMPC and absorption spectrum of A-melittin (—) in buffer (10 mM KPP, pH 7.4), both at 36°C. The emission spectrum was recorded at an excitation wavelength $\lambda_{ex} = 290$ nm with slits set at 4 nm, and the absorption spectrum with slits set at 3 nm.

Theory of FET for diffusion in two dimensions

The FET data in membranes were analyzed according to Wolber and Hudson (1979) who derived an analytical solution for FET in two dimensions which will be briefly summarized in the following. The fluorescence decay of the donor in the absence of acceptor is assumed to be mono-exponential,

$$I_0(t) = \exp(-t/\tau_0), \quad (5)$$

with the initial condition $I_0(t) = 1$. In the case of randomly diffusing donors and acceptors in two dimensions, the fluorescence decay is then given by the expression

$$I(t) = \exp\left[-t/\tau_0 - (t/\tau_0)^{1/3} a C_A\right] \quad (6)$$

with $a = 4.254$ and C_A denoting the number of acceptors in R_0^2,

$$C_A = R_0^2 c_A, \quad (7)$$

where c_A is the two-dimensional density of acceptors. Eq. 6 requires in addition R_0 to be much larger than R_e, the minimal distance between donors and acceptors. If this condition is fulfilled, the time dependence of $I(t)$, according to Eq. 6, can be used as a test for the free diffusion of donors and acceptors.

A second test is possible by studying the dependence of the intensity on the acceptor concentration C_A. For this purpose, Wolber and Hudson (1979) analyzed the steady-state intensity $I^{ss} = \int I(t)\,dt$ or the relative quantum yield,

$$\phi_r = \int I(t)\,dt / \int I_0(t)\,dt. \quad (8)$$

Inserting Eq. 6 and performing the integration, they obtained an analytical expression for ϕ_r. Furthermore, they showed in good approximation, that the dependence of ϕ_r on C_A can be described by

$$\phi_r = A_1 \exp(-k_1 C_A) + A_2 \exp(-k_2 C_A), \quad (9)$$

with $A_1 = 0.65, A_2 = 0.35, k_1 = 4.75, k_2 = 2.06$. The dependence of ϕ_r on the concentration of C_A is plotted in Fig. 2. Within the range $0 \le C_A \le 0.5$, the approximation differs by not more than 1% from the analytical solution.

Due to steric hindrance, donors and acceptors may not come into close contact, i.e., there may exist a finite exclusion radius R_e. Such an exclusion radius results in a modification of Eq. 6. However, this case could also be approximated by Eq. 9 and the corresponding parameters for some R_e/R_0 ratios were given by Wolber and Hudson (1979), leading to the curves included in Fig. 2.

An important point of this analysis of FET is that the relative quantum yield ϕ_r does not depend on the concentration of donors as long as their concentration C_D in R_0^2 is below 0.5. A deviation from this universal behavior occurs when part of the acceptors bind to donors. Then, the relative quantum yield is a sum of the relative quantum yields of unbound and bound donors

$$\phi_r^t = f^u \phi_r^u + f^b \phi_r^b, \quad (10)$$

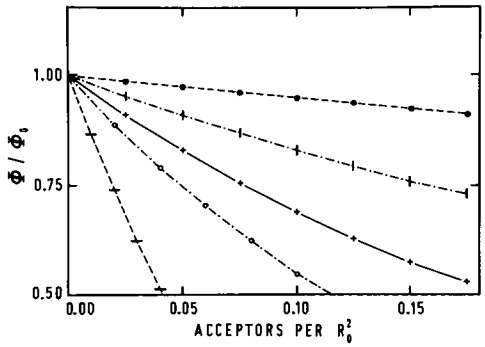

FIGURE 2 Decrease of the relative quantum yield due to FET in two dimensions, according to Eqs. 9 and 12, for different cases: (+) free diffusion and $R_e/R_0 = 0$, (|) free diffusion and $R_e/R_0 = 0.8$, (●) free diffusion and $R_e/R_0 = 1.3$, (○) binding with donor density $C_D = 0.5$, (−) binding with donor density $C_D = 0.1$. In the cases of binding we assumed $\phi_r^b = 0$ and $x = 1.0$ in Eq. 12.

with f^u and f^b denoting the fractions of unbound and bound donors so that $f^u + f^b = 1$. The relative quantum yield ϕ_r^u of unbound donors may be obtained from Eq. 9 with C_A given by the two-dimensional density of all acceptors. This implies that all acceptors, irrespective of being unbound or bound, participate in energy transfer from unbound donors. The relative quantum yield ϕ_r^b of bound donors may be obtained from Eq. 3.

In the case of not too high acceptor concentrations, $C_A \leq C_D$, one may assume the fraction of bound donors to be proportional to C_A/C_D (Wolber and Hudson, 1979) and to an additional factor x to account for a finite affinity between acceptors and donors,

$$f^b = x\frac{C_A}{C_D}. \tag{11}$$

Eq. 10 then becomes

$$\phi_r^t = \left(1 - x\frac{C_A}{C_D}\right)\phi_r^u + x\frac{C_A}{C_D}\phi_r^b. \tag{12}$$

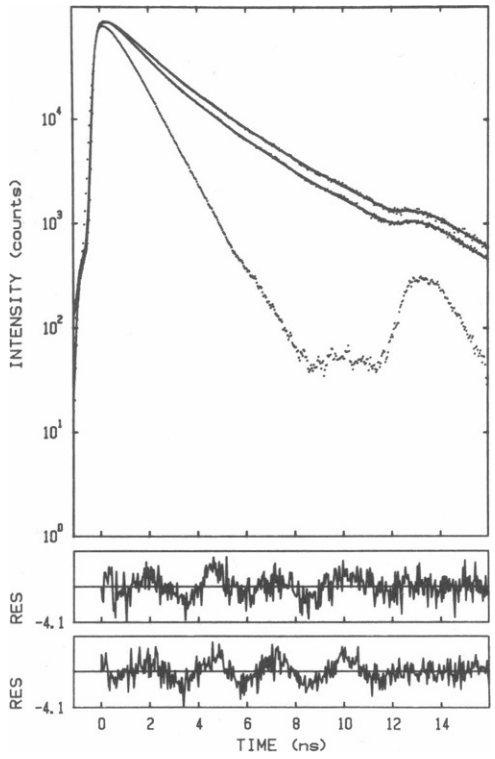

FIGURE 3 Intensity of the Trp fluorescence of 10 μM melittin in buffer (10 mM KPP, pH 7.4) with 2 M NaCl at 25°C. The experimental data (···) for the Trp intensities without and with A-melittin at an equimolar concentration to melittin and for the fast decaying fluorescence standard are shown in the upper part. Fits (—) of the Trp intensities are included. The corresponding residuals are shown in the lower part.

RESULTS

FET between melittin and A-melittin in water

As a test for FET between melittin and A-melittin, we performed time-resolved fluorescence measurement at a melittin concentration of 10^{-5} M in water at low and high ionic strength. Under these conditions, melittin is monomeric or tetrameric, respectively (Talbot et al., 1979; Quay and Condie, 1983). Fig. 3 shows the intensities of the Trp fluorescence at high ionic strength, without A-melittin and with A-melittin added equimolar to melittin. To facilitate the comparison, the two data sets were normalized to the same initial intensity. It is obvious that addition of A-melittin causes a faster decay of the Trp fluorescence. The results of fits by a sum of three exponentials are listed in Table 1. Three exponentials yielded a better fit than two exponentials, whereas four exponentials led to no further improvement. The values obtained without A-melittin are in agreement with earlier results (Georghiou et al., 1982; Tran and Beddard, 1985; Lakowicz et al., 1986; John and Jähnig, 1988). The value for the average life time $\bar{\tau}$ was almost identical using two, three, or four exponentials. However, for further analysis we always used the value obtained with three exponentials. The average lifetimes $\bar{\tau}_0 = 1.98$ ns and $\bar{\tau} = 1.63$ ns without and with A-melittin, respectively, lead to the relative quantum yield $\phi_r = \bar{\tau}/\bar{\tau}_0 = 0.82$. In Fig. 4, the relative quantum yields are plotted as a function of the concentration of A-melittin.

The relative quantum yields obtained at low ionic strength are included in Fig. 4. No significant FET could be detected in this case.

In analyzing these data, one has to keep in mind that in three dimensions, FET between randomly distributed donors and acceptors is negligible at concentrations

TABLE 1 **Results of fits of the intensity of the Trp fluorescence of 10 μM melittin in water with 2 M NaCl at 25°C, without A-melittin and at 10 μM A-melittin (data shown in Fig. 3)**

A-Melittin	0 μM		10 μM	
τ_1 (ns), α_1	0.81 ± 0.03	0.29 ± 0.03	0.67 ± 0.01	0.39 ± 0.02
τ_2 (ns), α_2	2.05 ± 0.07	0.58 ± 0.02	1.86 ± 0.04	0.51 ± 0.01
τ_3 (ns), α_3	4.33 ± 0.15	0.13 ± 0.01	4.11 ± 0.08	0.11 ± 0.01
$\bar{\tau}$ (ns)	1.98		1.63	
χ^2	1.95		2.32	

below $\sim 10^{-3}$ M (Förster, 1949). Hence, in our case this mechanism does not contribute and a finite FET indicates aggregation of donors and acceptors. At low ionic strength, melittin is monomeric and, accordingly, FET is not observed. At high ionic strength, melittin is tetrameric and gives rise to a considerable FET. Assuming the structure of the tetramer to be identical with the crystal structure of melittin (Terwilliger et al., 1982) and using Eq. 4 with R_0 = 26 Å to calculate the transfer efficiency within the tetramer, one obtains for the aggregation constant $K_4 = [M_4]/[M_1]^4 = 3 \times 10^{14}\ M^{-3}$. This value is comparable to the value $K_4 = 1.1 \times 10^{16}\ M^{-3}$ obtained by Quay and Condie (1983) at pH 7.

FET between melittin and DPH in lipid vesicle membranes

To study the case of a random distribution of donors and acceptors in lipid membranes, we performed FET measurements on melittin and DPH as donor/acceptor pair. DPH incorporates into the hydrophobic core of lipid membranes and is located at the end of the fatty acid chains of the lipids (Davenport et al., 1985). Due to its high absorbance around 360 nm, it is an appropriate acceptor for the Trp fluorescence of melittin. The average lifetime of the fluorescence of melittin in vesicle membranes of DMPC at 36°C and low ionic strength is $\bar{\tau}_0$ = 2.06 ns, in agreement with previous results (John and Jähnig, 1988). Addition of an equimolar amount of DPH decreases the average lifetime to $\bar{\tau}$ = 1.30 ns, leading to ϕ_r = 0.63. The data obtained at different DPH concentrations are included in Fig. 4. It is obvious from these data that in two-dimensional systems such as membranes a large FET may occur in the absence of aggregation, hence, a random distribution of donors and acceptors is sufficient to produce a large effect.

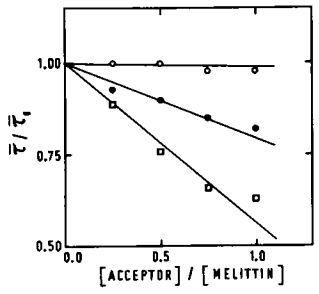

FIGURE 4 Plot of the ratio $\bar{\tau}/\bar{\tau}_0$ of the average fluorescence lifetime with and without acceptors versus the molar ratio of acceptor to donor melittin. The experimental conditions were: (○) 5-μM melittin in buffer without NaCl at 25°C with A-melittin as acceptor; (●) 10 μM melittin in buffer with 2 M NaCl at 25°C with A-melittin as acceptor; (□) 5-μM melittin in vesicle membranes of DMPC at 36°C and L/M = 200 with DPH as acceptor. Buffer in all cases was 10 mM KPP, pH 7.4.

FET between melittin and A-melittin in lipid vesicle membranes

The donor/acceptor pair melittin/A-melittin in vesicle membranes of DMPC at 36°C was investigated at low and high ionic strength and at different lipid/donor and lipid/acceptor mole ratios. Fig. 5 shows the intensities of the Trp fluorescence of melittin at high ionic strength and L/D = 200, without and with A-melittin at L/A = 500. The results of fits by a sum of three exponentials are listed in Table 2. The average lifetimes $\bar{\tau}_0$ = 2.44 ns[1] and $\bar{\tau}$ = 2.15 ns without and with A-melittin, respectively, lead to the relative quantum yield ϕ_r = 0.88.

To test whether this effect is caused by freely diffusing or by aggregated donors and acceptors, the deconvoluted fluorescence intensities $I_0(t)$ and $I(t)$ without and with A-melittin are plotted in Fig. 6 *A*, and the function $[ln[I_0(t)/I(t)]]^3$ is plotted in Fig. 6 *B*. According to Eq. 6, the latter function should yield a straight line if the FET arises from freely diffusing donors and acceptors. The experimental curve indeed follows a straight line closely, hence, the FET observed is caused predominantly by freely diffusing melittin and A-melittin molecules.

In the opposite case of aggregated donors and accep-

[1]That this number deviates somewhat from the above value 2.06 ns obtained without DPH is a consequence of sample preparation. Hence, only data obtained from one sample can be compared.

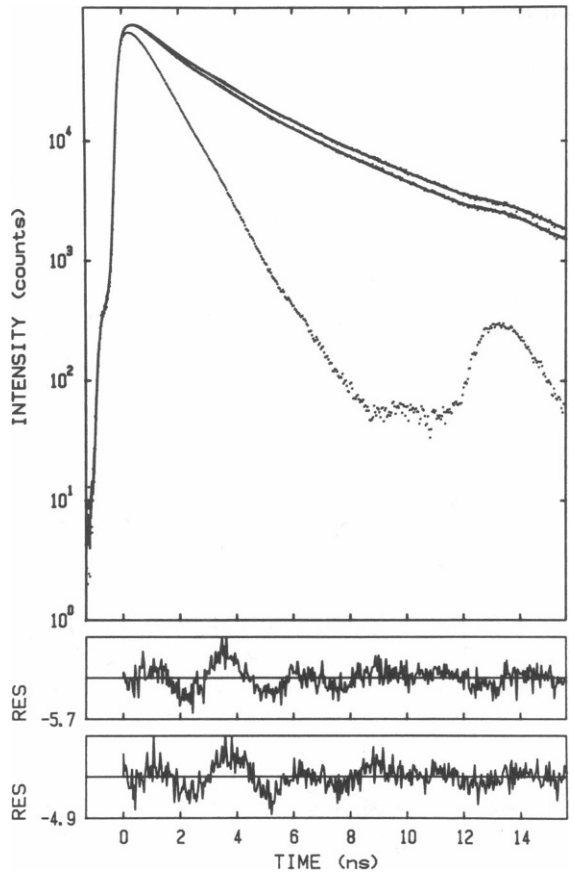

FIGURE 5 Intensity of the Trp fluorescence of 5-μM melittin in vesicle membranes of DMPC in buffer with 1 M NaCl at 36°C and $L/M = 200$. The experimental data (···) for the Trp intensities without and with A-melittin at $L/A = 500$, which corresponds to an acceptor density per R_0 of $C_A = 0.047$, and for the fast decaying fluorescence standard are shown in the upper part. Fits (—) of the Trp intensities are included. The corresponding residuals are shown in the lower part.

tors, the plot of Fig. 6 *B* should yield a cubic curve according to Eq. 4. This is demonstrated in Fig. 6 *B* (*dashed line*) where we have introduced the wrong assumption that the fluorescence intensities before and after the addition of A-melittin are monoexponential with lifetimes $\tau_0 = \bar{\tau}_0$ and $\tau = \bar{\tau}$, respectively (Fig. 6 *A*, *dashed lines*). Indeed, a cubic curve is obtained.

Further support for the notion that the FET observed at high ionic strength arises predominantly from randomly distributed donors and acceptors is obtained from the variation of the FET with donor and acceptor concentrations. In Fig. 7, the relative quantum yield is plotted as a function of the acceptor concentration C_A for different values of the donor concentration C_D. If the FET is caused by randomly distributed donors and acceptors, the data for all donor concentrations should lie on a universal curve according to Eq. 9. This is roughly found, but there is a slight difference between the curves for the L/D ratios 200, 500, and 1,000. In Table 3, we have listed the initial slopes $\Delta\phi_r/\Delta C_A$ of the various data sets as a measure for their difference. At high donor content, the relative quantum yield ϕ_r is lower and the slope $\Delta\phi_r/\Delta C_A$ larger. This is qualitative evidence that some aggregation takes place at high melittin content.

In an attempt to quantify this effect we assumed that at $L/D = 1{,}000$ or higher, no aggregation occurs. The initial slopes of the data were compared with the theoretical slopes for randomly distributed donors and acceptors to determine the exclusion radius R_e according to Eq. 9 and Fig. 2. Agreement was obtained for $R_e = 0.7$ $R_0 = 18$ Å. The data at $L/D = 200$ were then analyzed by permitting part of the melittin molecules to be aggregated according to Eq. 12. For the contribution to the FET from the random distribution of monomers and oligomers the exclusion radius $R_e = 18$ Å was used. For the oligomers we made the simple assumption of dimers with an acceptor/donor distance $R_i = R_e$ as lower limit (Wolber and Hudson, 1979). This led to a fraction $x = 0.12 \pm 0.03$ of aggregated melittin molecules. The error limit given here is derived from the uncertainty in the initial slope of the curves of Fig. 7. Upon variation of the exclusion radius within the range 15 Å $< R_e <$ 21 Å, the result for x stays within the given error limit. If, furthermore, the assumption of a dimer is released and replaced by the assumption of a tetramer made of four

TABLE 2 **Results of fits of the intensity of the Trp fluorescence of 5 μM melittin in vesicle membranes of DMPC at 1 M NaCl, without A-melittin and at $L/A = 500$ corresponding to $C_A = 0.047$**

C_A	0		0.047	
τ_1 (ns), α_1	0.61 ± 0.02	0.27 ± 0.02	0.53 ± 0.02	0.31 ± 0.01
τ_2 (ns), α_2	2.11 ± 0.05	0.48 ± 0.01	1.96 ± 0.04	0.47 ± 0.01
τ_3 (ns), α_3	5.06 ± 0.06	0.25 ± 0.01	4.83 ± 0.05	0.22 ± 0.01
$\bar{\tau}$ (ns)	2.44		2.15	
χ^2	2.49		1.90	

The molar lipid to melittin ratio was $L/D = 200$ (data shown in Fig. 5).

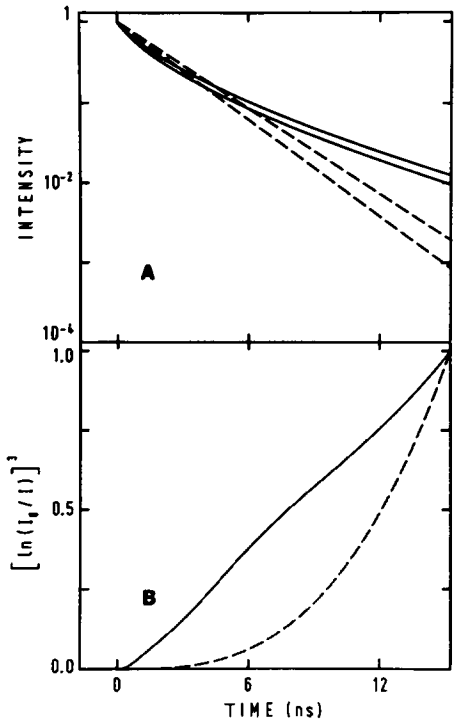

FIGURE 6 (*A*) Semi-logarithmic plots of the intensities described as a sum of three exponentials (—) using the parameters listed in Table 2. The upper curve corresponds to the case without A-melittin and the lower one to an A-melittin density C_A = 0.047. In addition, the corresponding single exponential decays are shown (----) using the averaged lifetimes $\bar{\tau}_0$ = 2.44 ns and $\bar{\tau}$ = 2.15 ns obtained without and with A-melittin. (*B*) Plots of the function $[ln(I_0/I)]^3$, with I_0 and I denoting the intensities without and with A-melittin, for the triple-exponential (—) and single-exponential (----) decays.

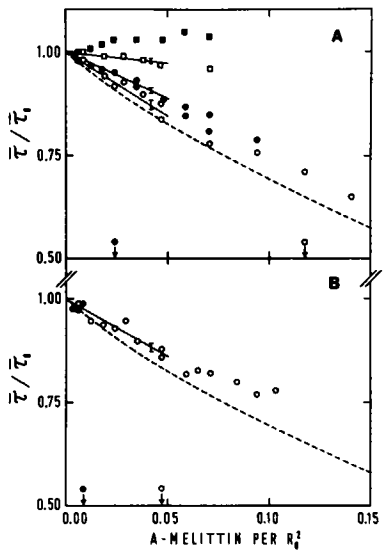

FIGURE 7 Plot of the ratio $\bar{\tau}/\bar{\tau}_0$ of the Trp fluorescence of 5-μM melittin in vesicle membranes of DMPC at 36°C versus the A-melittin density per R_0^2. The experimental conditions in (*A*) were: (■) *L/D* = 1,000 and 0 M NaCl; (●) *L/D* = 1,000 and 1 M NaCl; (□) *L/D* = 200 and 0 M NaCl; (○) *L/D* = 200 and 1 M NaCl. The broken line is the theoretical curve for a random distribution of donors and acceptors and an exclusion radius R_c = 0 (Eq. 9). The arrows mark the A-melittin densities where A-melittin was equimolar to melittin, i.e., (●) *L/A* = 1,000 and (○) *L/A* = 200. The experimental conditions in (*B*) were: (●) *L/D* = 3,000 and 1 M NaCl; (○) *L/D* = 500 and 1 M NaCl.

parallel membrane-spanning helices, the fraction of aggregated melittin molecules increases to x = 0.15, hence, is still within the given error limit. So our conclusion from this analysis is that of the order of 10% of the melittin molecules are aggregated in membranes of DMPC at high ionic strength. We cannot say anything, however, on the kind of aggregation, i.e., whether dimers or tetramers or other oligomers are formed.

Finally, the results on the FET at low ionic strength are included in Fig. 7. There is no evidence for an energy transfer in the range of the lipid/donor mole ratios investigated. This may be due to a relatively strong repulsion between melittin molecules at low ionic strength. At *L/D* = 1,000, there is even a slight increase of the relative quantum yield upon addition of A-melittin. This may be interpreted as a slight change in the exposure of melittin molecules to water upon increase of their concentration.

COMPARISON WITH DATA FROM THE LITERATURE

The FET studies on the aggregation of melittin in membranes which have been reported in the literature were steady-state measurements. The results of some of them are shown in Fig. 8 together with the results from our own steady-state measurements and our time-resolved measurements. Our steady-state measurements were performed at *L/D* = 1,000 and at low and high salt

TABLE 3 Initial slope $\Delta\phi_r/\Delta C_A$ of FET of the donor/acceptor pair melittin/A-melittin in vesicle membranes of DMPC at 36°C, at different ratios *L/D* and at 0 M and 1 M NaCl

L/D	[NaCl] (M)	$\Delta\phi_r/\Delta C_A$
3,000	1	−2.4 ± 0.9
1,000	1	−2.1 ± 0.1
500	1	−2.7 ± 0.2
200	1	−3.0 ± 0.2
1,000	0	+1.0 ± 0.2
200	0	−0.5 ± 0.1

$\Delta\phi_r/\Delta C_A$ was determined in the range $0 \leq C_A \leq 0.05$.

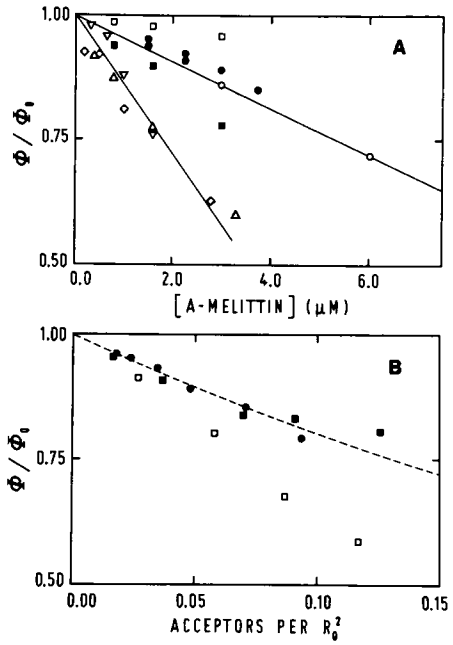

FIGURE 8. Comparison of different FET experiments. The data shown in (*A*) are: steady-state data of Vogel and Jähnig (1986) at low ionic strength, pH 4.5, and L/D = 9,410 (▽), L/D = 3,855 (◇) and L/D = 2,350 (△); steady-state data of Schwarz and Beschiaschvili (1989) at high and low ionic strength, pH 4.5, and L/D = 200 (○); our own steady-state data at high and low ionic strength, pH 5.0, and L/D = 1,000 (●); time-resolved data (shown in Fig. 7 *A*) at low (□) and high (■) ionic strength, pH 7.4, and L/D = 200. The lipid used was always DMPC at 30°C, except for Schwarz and Beschiaschvili (1989) who used DOPC at 20°C. The lines are drawn to guide the eye. The data shown in (*B*) are: Steady-state data of Talbot et al. (1987) at L/D = 3700 in egg PC (■) and DMPC (□) at 24°C; our own time-resolved data (shown in Fig. 7 *A*) at L/D = 1,000 in DMPC at 36°C (●). All data in (*B*) were recorded at high ionic strength. The broken line is the theoretical curve for a random distribution of donors and acceptors and an exclusion radius $R_e = 0.7\,R_0$ (Eq. 9).

concentration. No dependence on the salt concentration was observed. These data agree roughly with those of Schwarz and Beschiaschvili (1989) who also found no difference at low and high salt concentration. Their L/D ratio was 200, but this difference is of minor importance since the FET data lie approximately on a universal curve if the small contribution of aggregation at L/D = 200 is neglected for a moment. A considerably larger energy transfer was observed by Vogel and Jähnig (1986) at higher L/D ratios and low salt concentration. This was interpreted in terms of an aggregation of the melittin molecules. It is important to note, however, that all these steady-state measurements were performed at pH 4.5–5.0 in order to increase the overlap between emission of the donors and absorption of the acceptors. Under this condition, the acceptor A-melittin absorbs strongly also at the excitation wavelength of the donor (280 nm) and this may have caused the large effect observed by Vogel and Jähnig (1986).

This direct absorption by the acceptor molecules is difficult to correct and renders the steady-state measurements of Vogel and Jähnig (1986) and of Schwarz and Beschiaschvili (1989) questionable. It may also be the reason for the deviation between our steady-state data and our time-resolved data (Fig. 8 *A*). The latter was obtained at pH 7.4 but the protonation state of melittin should not differ between pH 5 and 7.4. The time-resolved measurements showed a pronounced salt effect. The FET at low salt concentration was lower than detected in the steady-state measurements, and at high salt concentration, was higher.

Such a strong salt effect was also observed by Talbot et al. (1987) in their steady-state measurements. As acceptor they used the oxidized Trp residue of melittin for which the absorption problem is less severe. Their measurements were performed at L/D = 3,700, pH 7.0, and low and high salt concentrations. Moreover, different lipids such as DMPC and egg PC were investigated at a temperature of 24°C. For DMPC, this corresponds to the ordered fluid phase transition, while egg PC is in the fluid phase. Hence, our time-resolved measurements on DMPC at 36°C and L/D = 1,000 or higher should be compared with their measurements on egg PC. They are indeed in good agreement. Talbot et al. (1987) interpreted their data as evidence for aggregation, but Fig. 8 *B* clearly shows that they lie on the same universal curve for randomly distributed donors and acceptors with $R_e = 0.7\,R_0$ as the time-resolved data for L/D = 1,000. Therefore, they should also be interpreted as a consequence of a random distribution of donors and acceptors. Only a deviation from the universal curve as observed in our time-resolved measurements at L/D = 200 can be taken as evidence for aggregation.

CONCLUSION

By time-resolved FET measurements, we could show that melittin in fluid membranes of DMPC is predominantly monomeric. Only at melittin/lipid ratios of 1/200 or higher and high salt concentration, an indication for aggregation was found, the percentage of aggregated melittin molecules being of the order of 10% at L/D = 200 and 1 M NaCl. Previous reports on a strong aggregation of melittin in membranes, which were based on steady-state measurements, suffer either from high direct absorption of the acceptors (Vogel and Jähnig, 1986) or from misinterpretation of the data (Talbot et al., 1987). Our result on a predominant monomeric state

of melittin in membranes is in consonance with results obtained by other techniques such as NMR (Stanislawski and Rüterjans, 1987) and ESR (Altenbach and Hubbell, 1988).

Supposedly, melittin monomers lie more or less flat on the membrane surface with the hydrophobic side of the melittin helix making contact with the hydrophobic core of the lipid bilayer. In the aggregated state, the melittin helices are supposed to be shifted towards the hydrophobic core and become oriented more along the membrane normal with the hydrophobic side still facing the lipids. This would give rise to a polar pore in the membrane (Vogel and Jähnig, 1986). Between the two states, there would be a dynamic equilibrium, which, under the condition of low melittin concentration or low salt concentration lies completely on the monomeric state. Only at high melittin content and high salt concentration, a small shift towards the aggregated state is observed. A membrane potential, however, may act on the helix dipoles and, if transnegative, orient them more along the membrane normal (Kempf et al., 1982) so that the equilibrium would be shifted more towards the aggregated state. In this way, the action of melittin as a voltage-gated pore might be explained. This proposal corresponds closely to the model proposed for alamethicin by Fox and Richards (1982). Certainly, more experimental data, especially on the structure of melittin in other lipids and in the presence of a membrane potential, are required to solve the problem of melittin in membranes completely.

Received for publication 19 October 1990 and in final form 27 March 1991.

REFERENCES

Altenbach, C., and W. L. Hubbell. 1988. The aggregation state of spin labeled melittin in solution and bound to phospholipid membranes: evidence that membrane-bound melittin is monomeric. *Proteins.* 3:230–242.

Bazzo, R., M. J. Tappin, A. Pastore, T. S. Harvey, J. A. Carver, and I. D. Campbell. 1988. The structure of melittin. A ^{1}H-NMR study in methanol. *Eur. J. Biochem.* 173:139–146.

Best, L., E. John, and F. Jähnig. 1987. Order and fluidity of lipid membranes as determined by fluorescence anisotropy decay. *Eur. Biophys. J.* 15:87–102.

Brauner, J. W., R. Mendelsohn, and F. G. Prendergast. 1987. Attenuated total reflectance Fourier transform infrared studies of the interaction of melittin, two fragments of melittin, and δ-hemolysin with phosphatidylcholines. *Biochemistry.* 26:8151–8158.

Dale, R. E., and J. Eisinger. 1974. Intramolecular distances determined by energy transfer. Dependence on orientational freedom of donor and acceptor. *Biopolymers.* 13:1573–1605.

Davenport, L., R. E. Dale, R. H. Bisby, and R. B. Cundall. 1985. Transverse location of the fluorescent probe 1,6-diphenyl-1,3,5-hexatriene in model lipid bilayer membrane systems by resonance excitation energy transfer. *Biochemistry.* 24:4097–4108.

Dempsey, C. E. 1990. The action of melittin on membranes. *Biochim. Biophys. Acta.* 1031:143–161.

Eisinger, J. 1969. A variable temperature, U.V. luminescence spectrograph for small samples. *Photochem. Photobiol.* 9:247–258.

Fairclough, R. H., and C. R. Cantor. 1978. The use of singlet–singlet energy transfer to study macromolecular assemblies. *Methods Enzymol.* 48:347–379.

Förster, T. 1949. Experimentelle und theoretische Untersuchung des zwischenmolekularen Übergangs von Elektronenanregungsenergie. *Z. Naturforsch.* A4:321–327.

Fox, R. O., and F. M. Richards. 1982. A voltage-gated ion channel model inferred from the crystal structure of alamethicin at 1.5 Å resolution. *Nature (Lond.).* 300:325–330.

Georghiou, S., M. Thompson, and A. K. Mukhopadhyay. 1982. Melittin-phospholipid interaction studied by employing the single tryptophan residue as an intrinsic fluorescent probe. *Biochim. Biophys. Acta.* 688:441–452.

Habermann, E., and H. Kowallek. 1970. Modifikation der Aminogruppen und des Tryptophans im Melittin als Mittel zur Erkennung von Struktur-Wirkungs-Beziehungen. *Hoppe-Seyler's Z. Physiol. Chem.* 351:884–890.

Hermetter, A., and J. R. Lakowicz. 1986. The aggregation state of melittin in lipid bilayers. *J. Biol. Chem.* 26:8243–8248.

Horton, H. R., and D. E. Koshland. 1967. Reactions with reactive alkyl halides. *Methods. Enzymol.* 11:556–565.

Inagaki, F., J. Shimada, K. Kawaguchi, M. Hirano, J. Terasawa, T. Ikura, and N. Go. 1989. Structure of melittin bound to perdeuterated dodecylphosphocholine micelles as studied by two-dimensional NMR and distance geometry calculations. *Biochemistry.* 28:5985–5991.

John, E., and F. Jähnig. 1988. Dynamics of melittin in water and in membranes as determined by fluorescence anisotropy decay. *Biophys. J.* 54:817–827.

Kempf, D., R. D. Kausner, J. H. Weinstein, J. van Renswoude, M. R. Pincus, and R. Blumenthal. 1982. Voltage-dependent transbilayer orientation of melittin. *J. Biol. Chem.* 257:2469–2476.

Lakowicz, J. R., C. Laczko, J. Gryczynski, and H. Cherek. 1986. Measurement of subnanosecond anisotropy decay of protein fluorescence using frequency-domain fluorometry. *J. Biol. Chem.* 261:2240–2245.

Quay, S. C., and C. C. Condie. 1983. Conformational studies of aqueous melittin: thermodynamic parameters of the monomer-tetramer self-association reaction. *Biochemistry.* 22:695–700.

Schwarz, G., and G. Beschiaschvili. 1989. Thermodynamic and kinetic studies on the association of melittin with a phospholipid bilayer. *Biochim. Biophys. Acta.* 979:82–90.

Stanislawski, B., and H. Rüterjans. 1987. ^{13}C-NMR investigation of the insertion of the bee venom melittin into lecithin vesicles. *Eur. Biophys. J.* 15:1–12.

Talbot, J. C., J. Dufourcq, J. de Bony, J. F. Faucon, and C. Lussan. 1979. Conformational change and self-association of monomeric melittin. *FEBS (Fed. Eur. Biochem. Soc.) Lett.* 102:191–193.

Talbot, J. C., J. F. Faucon, and J. Dufourcq. 1987. Different states of self-association of melittin in phospholipid bilayers. *Eur. Biophys. J.* 15:147–157.

Terwilliger, T. C., L. Weissman, and D. Eisenberg. 1982. The structure of melittin in the form I crystals and its implications for melittin's lytic and surface activities. *Biophys. J.* 37:353–361.

Tran, C. D., and G. S. Beddard. 1985. Studies of the fluorescence from tryptophan in melittin. *Eur. Biophys. J.* 13:59–64.

Vogel, H. 1987. Comparison of the conformation and orientation of Alamethicin and Mellitin in lipid membranes. *Biochemistry.* 26:4562–4572.

Vogel, H., and F. Jähnig. 1986. The structure of melittin in membranes. *Biophys. J.* 50:573–582.

Wille, B. 1989. A preparation of melittin depleted of phospholipase A2 by ion exchange chromatography in denaturing solvents. *Anal. Biochem.* 178:118–120.

Wolber, P. K., and B. S. Hudson. 1979. An analytical solution to the Förster energy transfer problem in two dimensions. *Biophys. J.* 28:197–210.